Journal of Alloys and Compounds 505 (2010) 472–475

Contents lists available at ScienceDirect

Journal of Alloys and Compounds

journal homepage: www.elsevier.com/locate/jallcom

Effect of liquid–liquid structure transition on solidification and wettability of Sn–0.7Cu solder

Xianfen Li*, Fei Zhang, Fangqiu Zu, Xue Lv, Zhenxing Zhao, Dongdong Yang

School of Materials Science and Engineering, Hefei University of Technology, Hefei 230009, China

ARTICLE INFO

Article history:
Received 13 January 2010
Received in revised form 6 June 2010
Accepted 12 June 2010
Available online 25 June 2010

Keywords:
Sn–0.7Cu solder
Liquid–liquid structure transition
Solidification
Wettability

ABSTRACT

The temperature dependence of electrical resistivity (ρ–T) of a Sn–0.7Cu (wt.%) melt was measured and an abnormal change was found on the ρ–T curve within the range of 825–1066 °C. The result suggests that the melt has experienced a temperature-induced liquid–liquid structural transition (TI-LLST), and the transition is reversible after the first cycle heating. Based on the result of TI-LLST, solidification experiments and spreadability tests were carried out on the Sn–0.7Cu alloy to investigate the effect of liquid structure transition on solidification microstructure and wettability. The results show that the microstructure was refined and the wettability was improved when the samples solidified from the melt experienced TI-LLST.

1. Introduction

Due to the hereditary effects of liquid on solid, the thermal history of melt has a great effect on the microstructures and properties of as-cast materials. Melt thermal treatment and melt superheating treatment have been widely explored and used in modifying the solidification microstructure and improving the mechanical or physical properties of various materials: metallic alloys [1–5], aerogel [6], and polyethylene [7]. But the exact mechanism is still not fully understood and there are discrepancies in the explanations put forward [8].

In recent years, liquid–liquid transition has attracted much attention in liquid physics and materials field. And many experimental and theoretical studies have shown that temperature-induced or pressure-induced liquid–liquid structural transition can occur in some single-component and multiple-components liquids [9–14]. In our previous work, temperature-induced liquid–liquid structural transitions (TI-LLSTs) have been observed in some binary alloys, such as In–Sn, In–Bi, Pb–Sn, Cu–Sn and Pb–Bi, by the electrical resistivity method [15–17], X-ray diffraction [18,19], revised internal friction method [20], and differential scanning calorimetry (DSC) [21]. Compared with other experiments, electrical resistivity experiment is a relative simple but effective method to investigate liquid structure changes due to the fact that electrical resistivity is a sensitive physical property to structures.

It has been widely accepted that the traditional Sn–Pb solders should be substituted by lead-free solders, because of the hazard of lead on environment and human health. Among the main Sn-base lead-free solders such as Sn–Ag, Sn–Cu, Sn–Ag-Cu, Sn–Zn, and Sn–Bi alloys, Sn–0.7Cu alloy has been recognized as one of the leading lead-free solder candidates due to its low material cost [22–24]. Thus it is useful to explore the effect of melt structural transition on the solidification and properties of Sn–0.7Cu alloy.

In this article, the temperature dependence of electrical resistivity on the liquid Sn–0.7Cu alloy was investigated, and the results suggest that a reversible structural change occurs in a relatively high-temperature range. And the effect of TI-LLST on the solidification microstructure and wettability was also discussed, which may lead to a better understanding of the nature of TI-LLST and its effect on solidification microstructure and wettability.

2. Experimental procedures

2.1. Electrical resistivity measurements

The electrical resistivity measurements were carried out by means of direct current four-probe technology. The details of the measuring method are the same as described elsewhere [15]. The Sn–0.7Cu (wt.%) sample was prepared with tin and copper granules of high purity (4N). The melt was heated to 400 °C, and held for 1 h covered with KCl–LiCl melts, then poured into a quartz cells and cooled to a temperature below liquidus (227 °C) for the following experiments. During the entire melting process, the sample was shaken mechanically three times for component homogenization. In the resistivity measurements, the heating and cooling rate were both 5 °C/min, and the ρ–T curve was recorded by a computer datum collection system. The thermal expansion of the quartz was so small that the size variation with temperature could be neglected.

* Corresponding author. Tel.: +86 551 2905057.
E-mail address: lxfytt@163.com (X. Li).

0925-8388/$ – see front matter © 2010 Elsevier B.V. All rights reserved.
doi:10.1016/j.jallcom.2010.06.087

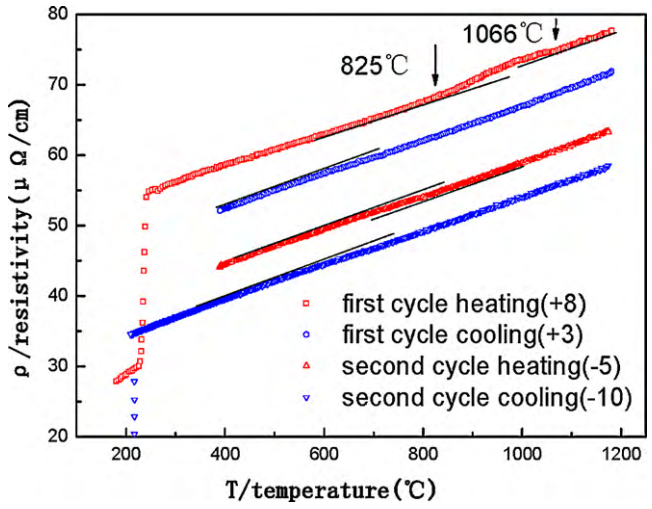

Fig. 1. Electrical resistivity–temperature curves of Sn–0.7Cu alloy in two heating and cooling cycles. (Note: in order to observe the ρ–T curves in different cycles, the ordinate value ρ is added with a different value as listed in the inset brackets.)

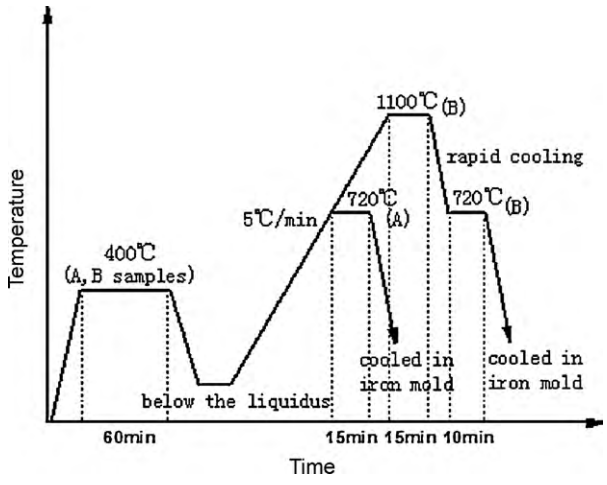

Fig. 2. Sketch of preparation procedure of liquid Sn–0.7Cu alloys.

2.2. Solidification experiments

In the experiments, the melting and holding temperatures of the alloys are chosen according to the ρ–T curve, which is shown in Fig. 1. In addition, the temperature treatments of the liquid alloys were conducted in accordance with the following sequential scheme (Fig. 2): two same weight Sn–0.7Cu samples A and B (20.000 g) were heated and held at 400 °C for 1 h covered with B_2O_3 (to avoid the evaporation and oxidation), and then cooled down. Sample A was then heated to 720 °C (before the liquid change temperature of the first heating cycle) and held for 15 min, and then poured into an iron mold. Sample B was heated to 1100 °C (above the temperature range with the anomalous change) and held for 15 min, and then rapidly cooled to 720 °C. At 720 °C, it was held for another 10 min, and finally poured into the same iron mold.

The solidified sample was divided into two parts: One was used to analyze the microstructures; the other was used for wettability tests. The specimens for microstructures were prepared by standard metallographic procedures with a solution of $FeCl_3$ + HCl + H_2O as the etchant and observed under optical microscope (OM).

2.3. Wettability tests

In order to examine the effect of liquid structural transition on wettability, spreadability tests were carried out. According to the National Standard of China GB/T 11364-2008 "Testing Method of wettability for brazing filler metals", the substrate used was copper with a purity of 99.97 wt.%, which was cut into the size of 40 mm × 40 mm × 2 mm. The Cu substrate was polished with 600-grit sandpaper before cleaning with ethanol. The solder wafer was cut into 0.2 ± 0.0002 gram (using an electronic balance) with the same diameter. Spreadability tests were conducted at 260 °C with a dwelling time of 60 s in a resistance furnace, and activated rosin was used as flux. Spreading areas of the solders on Cu surface were measured by using an optical microscope.

3. Results and discussions

3.1. Electrical resistivity

Fig. 1 shows the ρ–T curve of the Sn–0.7Cu melt. The resistivity of the melt increases linearly with temperature rising above the liquidus; however, it changes abruptly from 825 °C to 1066 °C; then increases linearly again above 1066 °C. The anomalous changes are reversible in subsequent cooling and heating process, but the turning points and the change trend are different from that of the first cycle heating. It is presumed that two types of TI-LLST exist in Sn–0.7Cu melt, i.e. irreversible TI-LLST in the first cycle heating and reversible after the first cycle heating.

It is generally agreed that the atomic bonds of crystals are only partly broken on melting, and the liquid structures are mainly composed of atomic clusters and a few free atoms [25,26]. According to ref. [27], high temperature X-ray diffractometer had been used to study the liquid structure of Sn–0.7Cu alloy, and the experimental result showed that only short-range orders (SROs) were detected in molten Sn–0.7Cu alloy at 260, 330, 400 °C. In addition, investigations of the high-temperature properties and SROs of melts showed that the microheterogeneous states were metastable or nonequilibrium rather than thermodynamically stable [28]. Accordingly, in this study, we can reasonably deduce that there are probably many metastable SROs (such as Sn–Sn, Cu-Cu and Sn–Cu SROs) in the melt at a low temperature above the liquidus. With the temperature rising, those metastable SROs dissolve or break into stable SROs within the temperature range of 825–1066 °C. Then the melt becomes more uniform and disorder. This metastable to stable transition in the Sn–0.7Cu melt is irreversible.

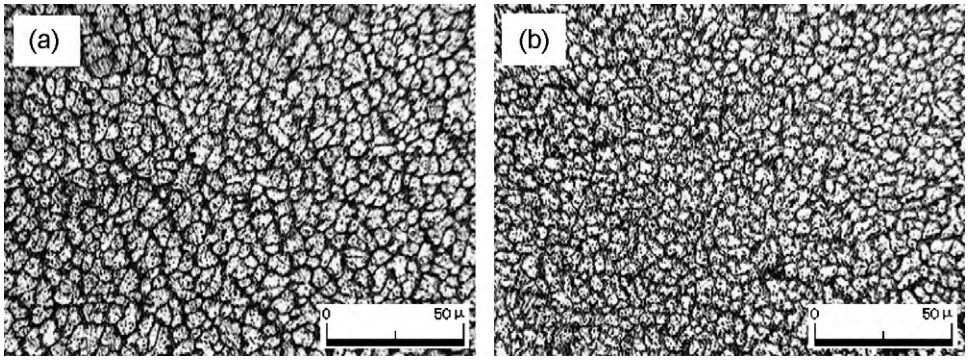

Fig. 3. Solidification microstructures of Sn–0.7Cu alloy: (a) for sample A and (b) for sample B.

Table 1
Spreadability of solders on Cu substrate (260 °C, 60 s).

Solders	Sample A	Sample B	The relative variable ratio of sample B as against sample A
Spreading area (mm^2)	45.467	49.969	+9.90%
Wetting angle (°)	33.008°	31.775°	−3.74%

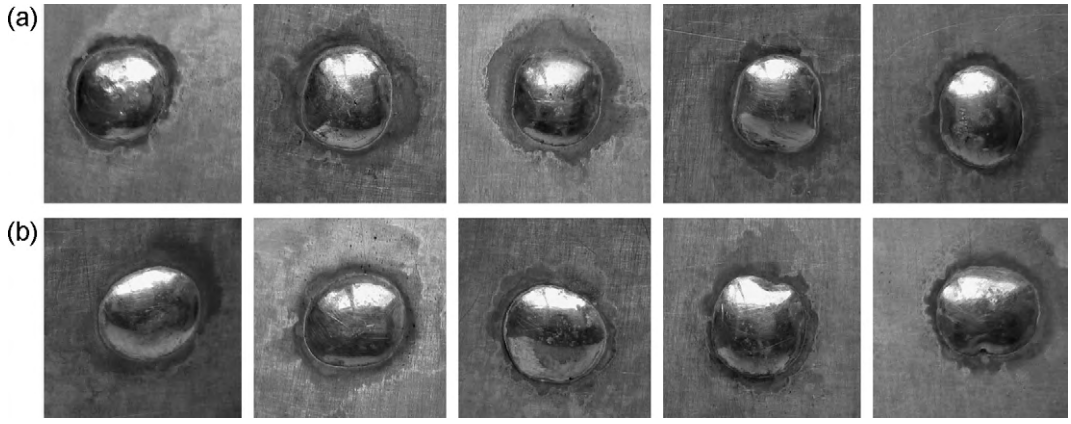

Fig. 4. Spreadability testing of solders: (a) for sample A and (b) for sample B.

In respect to the different characteristic of the anomaly on ρ–T curves between the first heating cycle and the subsequent cycles, we can assume that the stable Sn–0.7Cu melt has some SROs with reversible change character, i.e. they can reassemble on cooling and break again on heating. According to ref. [29], the liquid structure of Sn has been investigated by neutron scattering experiments. The experimental result showed that an obvious shoulder exists on the high-Q side of the first peak of S (Q) at 300 °C, 500 °C, and even 1600 °C. Since the shoulder is a sign of a covalent bond, these features for liquid Sn suggest that some tetrahedral SROs with covalent characteristics may remain in liquid Sn at lower temperatures, and at least the fragments of tetrahedral unit could persist at high temperatures in liquid Sn. In addition, comparing the results of ref. [27] with that of the liquid structure of Sn in ref. [30], it can be inferred that the liquid structure of Sn–0.7Cu solder is similar to that of Sn in a low-temperature range above liquidus. It is reasonable to presume that the tetrahedral SROs with covalent characteristic in liquid Sn and Sn–0.7Cu melt may be the main cause of the reversible TI-LLST.

3.2. Solidification microstructure

The microstructure of samples A and B are shown in Fig. 3. According to ref. [31], only β-Sn and Cu_6Sn_5 phases exist in the solidified Sn–0.7Cu alloy. From the observation of microstructure, the microstructure of the rapidly cooled Sn–0.7Cu alloy has light regions of β-Sn grains and dark regions of eutectic colonies containing Cu_6Sn_5 intermetallic compounds (IMCs). From Fig. 3, we can see that, although the two samples were cooled down from the same condition, the microstructures become finer when solidified from the melt experienced the TI-LLST (sample B).

The Sn–0.7Cu melt which did not undergo the TI-LLST has lots of relatively big-size clusters. Through fluctuations in structure and energy, those clusters can easily reach the critical nucleation radius so that they can nucleate under a low under-cooling. Up to the TI-LLST temperature, the big-size clusters absorb enough energy to disintegrate into smaller ones or break up; as a result, the melt becomes absolutely disordered and homogeneous. On this condition the melt needs a greater under-cooling to nucleate. Furthermore, with greater under-cooling degree, the density of critical size nucleus and the nucleating rate would be higher while the growth rate becomes slower due to lower atom diffusion rate. Analysis from the both points of nucleating and growing, the solidification structure would be finer when solidifying from the melt which experienced TI-LLST.

3.3. Wettability

The results of the spreadability testing of the solders are shown in Table 1 and Fig. 4. The spreadability testing samples in Fig. 4(a) are from the solders (sample A) before the TI-LLST, and the solders (sample B) used in Fig. 4(b) are solidified from the melt experienced the TI-LLST. It can be found that the overall spreading area in Fig. 4(b) is larger than that of Fig. 4(a). Compared with that of sample A, the spreading area of sample B increased by 9.90%, while the wetting angle decreased by 3.74% (as seen in Table 1).

During the soldering process, the wetting interaction was dominated by three surface energies: the surface energy of the substrate/flux γ_{SF}, the surface energy of the substrate/liquid solder interfacial area γ_{SL}, and the surface energy of the liquid solder/flux γ_{LF}. The equilibrium contact angle θ_{eq} is defined by the Young–Dupre equation [32]:

$$\cos\theta_{eq} = \frac{\gamma_{SF} - \gamma_{SL}}{\gamma_{LF}} \quad (1)$$

γ_{SF} is determined by the structures of the substrate and flux, so γ_{SF} may be regarded as constant. γ_{SL} and γ_{LF} are determined by the property of the molten alloy. The melt which experienced TI-LLST is more disordered and homogeneous than the melt did not experience, so atoms in the former state are more active as compared to that of the latter. Therefore, when sample B started to melt and spread as the temperature increased, it was easy to spread on the Cu substrate due to the higher atoms' activity. In addition, γ_{SL} and γ_{LF}, which prevent molten alloy from spreading on the Cu substrate, decrease as a result of increased atoms' activity. According to Eq. (1), the equilibrium contact angle then decreases, and the wettability is improved when the melt has experienced TI-LLST.

3.4. Shear strength

According to the standard of soldered joint's shear strength, some soldered joints were obtained using the solidified solders

Table 2
Shear strength of the soldered joint (MPa).

Samples	1	2	3	Average value	Change rate of B against A
Sample A	43.333	43.773	43.741	43.616	
Sample B	45.432	45.990	46.268	45.897	+5.23%

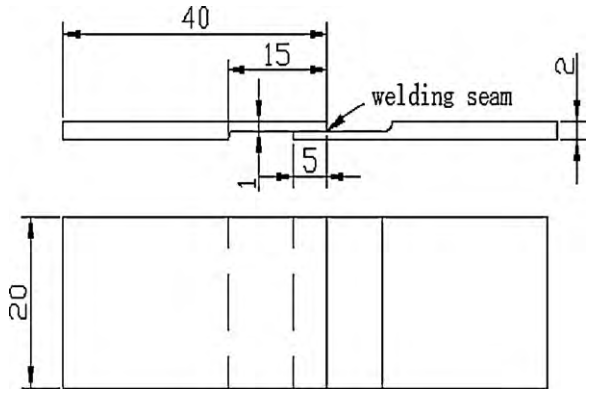

Fig. 5. Schematic figure of the soldered joint in the shear strength testing.

(samples A and B), and Cu plate as substrate (shown in Fig. 5). The results of shear strength testing are listed in Table 2. From Table 2, it can be found that the shear strength of sample B joint (after the TI-LLST) is about 5.23% higher than that of the sample A (before the TI-LLST). The result of shear strength testing is consistent with the result of the wettability test.

4. Conclusions

The following conclusions are drawn from the results of the investigation:

(1) The anomalous change on the ρ–T curve suggests that there are two sorts of TI-LLSTs in the Sn–0.7Cu melt—irreversible in the first cycle heating and reversible in the subsequent cycles. The irreversible TI-LLST can be attributed to the metastable to stable transition of SROs, and the reversible TI-LLST is closely related to the tetrahedral SROs with covalent characteristic. And the structural transition results in a more disordered melt which has an obvious effect on solidification and wettability.
(2) The disordered melt inhibits the nucleation because of the homogeneous and smaller size clusters; thus the melt needs a high under-cooling to nucleate, and a higher nucleation rate will be obtained. In addition, greater under-cooling degree inhibits the crystal growth of the primary phase owing to low atom diffusion rate. Eventually, the TI-LLST refines the solidification microstructures.
(3) For the disordered melt after TI-LLST, the surface energies of γ_{SL} and γ_{LF} decrease due to the higher atoms' activity; so the equilibrium contact angle decreases and the spreading area on the Cu substrate increases to improve the wettability of the Sn–0.7Cu solder, and the shear strength of soldered joints increases correspondingly.

Acknowledgments

This work was supported by the National Natural Science Foundation of China (No. 50571033), and by the Natural Science Foundation of Anhui Province (No. 070414178 and No. 070416234), and HFUT Research and Development Funds (No. 2007GDBJ016).

References

[1] M. Johnsson, L. Backerud, Z. Metallkd. 83 (1992) 774–780.
[2] J. Zengyun, Y. Gengcang, Z. Yaohe, Trans. Nonferr. Met. Soc. Chin. 5 (1995) 133–135.
[3] H. Chiriac, F. Vinai, M. Tomut, A. Stantero, E. Ferarra, J. Non-Cryst. Solids 250–152 (1999) 709–713.
[4] X.F. Bian, W.M. Wang, Mater. Lett. 44 (2000) 54–58.
[5] F.S. Yin, X.F. Sun, J.G. Li, H.R. Guan, Z.Q. Hu, Scripta Mater. 48 (2003) 425–429.
[6] D.R. Vollet, D.A. Donatti, A. Ibanez Ruiz, W.C. de Castro, J. Non-Cryst. Solids 332 (2003) 73–79.
[7] L.M.W.K. Gunaratne, R.A. Shanks, G. Amarasinghe, Thermochim. Acta 423 (2004) 127–135.
[8] D. Qiu, M.X. Zhang, J.A. Taylor, H.M. Fu, P.M. Kelly, Acta Mater. 55 (2007) 1863–1871.
[9] S. Aasland, P. McMillan, Nature 369 (1994) 633–636.
[10] S. Harrington, R. Zhang, P.H. Poole, F. Sciortino, H.E. Stanley, Phys. Rev. Lett. 78 (1997) 2409–2412.
[11] P. McMillan, Nature 403 (2000) 151–152.
[12] P.H. Poole, T. Grande, C.A. Angell, P.F. McMillan, Science 275 (1997) 322–323.
[13] M.V. Coulet, C. Bergman, R. Bellissent, C. Bichara, J. Non-Cryst. Solids 250–252 (1999) 463–467.
[14] A.K. Soper, M.A. Ricci, Phys. Rev. Lett. 84 (2000) 2881–2884.
[15] F.Q. Zu, X.F. Li, H.F. Ding, G.H. Ding, Phase Transit. 79 (2006) 277–283.
[16] X.F. Li, F.Q. Zu, L.J. Liu, J. Yu, B. Zhou, Phys. Chem. Liq. 45 (2007) 531–539.
[17] F.Q. Zu, R.R. Shen, Y. Xi, X.F. Li, G.H. Ding, H.M. Liu, J. Phys. Condens. Matter 18 (2006) 2817–2823.
[18] F.Q. Zu, Z.G. Zhu, L.J. Guo, X.B. Qin, H. Yang, W.J. Shan, Phys. Rev. Lett. 89 (2002) 125505.
[19] F.Q. Zu, X.F. Li, L.J. Guo, H. Yang, X.B. Qin, Z.G. Zhu, Phys. Lett. A 324 (2004) 472–478.
[20] F.Q. Zu, Z.G. Zhu, B. Zhang, Y. Feng, J.P. Shui, J. Phys. Condens. Matter 13 (2001) 11435–11442.
[21] J. Chen, F.Q. Zu, X.F. Li, G.H. Ding, H.S. Chen, L. Zhou, Met. Mater. Int. 14 (2008) 569–574.
[22] K. Suganuma, Curr. Opin. Solid State Matter 5 (2001) 55–64.
[23] S.K. Kang, A.K. Sarkhel, J. Electron. Mater. 23 (1994) 701–707.
[24] B. Trumble, IEEE Spectrom. 35 (1998) 55–60.
[25] H. Richter, G. Breitling, Z. Metalkd. 61 (1970) 628–636.
[26] A.C. Mitus, A.Z. Patashinkii, B.I. Shumilo, Phys. Lett. A 113 (1985) 41–44.
[27] N. Zhao, X.M. Pan, H.T. Ma, L. Wang, Acta Metall. Sin. 44 (2008) 467–472.
[28] P.S. Popel, O.A. Chikova, V.M. Matveev, High Temp. Mater. Proc. 14 (1995) 219–233.
[29] T. Itami, S. Munejiri, T. Masaki, H. Aoki, Y. Ishii, T. Kamiyama, Y. Senda, F. Shimojo, K. Hoshino, Phys. Rev. B 67 (2003) 064201.
[30] J.Y. Qin, X.F. Bian, W.M. Wang, Acta Phys. Sin. 47 (1998) 438–444.
[31] J. Shen, Y. Liu, H. Gao, J. Univ. Sci. Technol. Beijing 13 (2006) 333–337.
[32] A.W. Adamson, Physical Chemistry of Surfaces, 5th ed., Wiley, New York, 1990.